Received: 2 October 2020 | Revised: 4 November 2020 | Accepted: 9 November 2020

DOI: 10.1002/ansa.202000123

ANALYTICAL SCIENCE ADVANCES

WILEY-VCH

FULL ARTICLE

Quadrupole detection FT-ICR mass spectrometry offers deep profiling of residue oil: A systematic comparison of 2ω 7 Tesla versus 15 Tesla instruments

Jinfeng Ge[1,#] | Chao Ma[1,#] | Yulin Qi[1,2] | Xiaowei Wang[3] | Wei Wang[3] | Miao Hu[4] | Qiaozhuan Hu[1] | Yuan-Bi Yi[1] | Dejun Shi[5] | Fu-Jun Yue[1,2] | Si-Liang Li[1,2] | Dietrich A. Volmer[6]

[1] Institute of Surface-Earth System ScienceSchool of Earth System ScienceTianjin University, Tianjin, China

[2] Tianjin Key Laboratory of Earth Critical Zone Science and Sustainable Development in Bohai Rim, Tianjin University, Tianjin, China

[3] Analytical Chemistry Department, Research Institute of Petroleum Processing (RIPP), Sinopec, Beijing, China

[4] CNOOC Research Institute of Refining and Petrochemicals, Beijing, China

[5] Petrochina Petrochemical Research Institute, Beijing, China

[6] Department of Chemistry, Humboldt-Universität zu Berlin, Berlin, Germany

Correspondence
Yulin Qi, Institute of Surface-Earth System Science, School of Earth System Science, Tianjin University, Tianjin, China.
Email: yulin.qi@tju.edu.cn

[#]These authors contributed equally to this work.

Funding information
National Natural Science Foundation of China, Grant/Award Numbers: 42007290, 41925002; Deutsche Forschungsgemeinschaft, Grant/Award Number: DFG VO 1355/4-3

Abstract

Mass resolving power is one of the key features of Fourier transform ion cyclotron resonance mass spectrometry (FT-ICR MS), which enables the molecular characterization of complex mixtures. Quadrupole (2ω) detection provides a significant step forward in FT-ICR MS performance, as it doubles the resolving power for a given signal acquisition time. Whether this 2ω detection technique truly substitutes for a higher magnetic field remains unknown however. In this study, a residue oil sample was characterized using both a 2ω 7 Tesla FT-ICR and a 15 Tesla FT-ICR instrument, and analytical figures of merit were systematically compared. It was shown that 2ω 7T FT-ICR MS provided comparable performance in the deep profiling of the complex oil sample, with better signal intensities and reproducibilities for absorption-mode processing. The 15T FT-ICR MS gave more precise measurements with better estimates of the sample's elemental compositions. To the best of our knowledge, this is the first published study, which thoroughly compared the performance of 2ω detection on a low magnetic field instrument with that of a high magnetic field FT-ICR-MS.

KEYWORDS
FT-ICR MS, quadrupole detection, residue oil, resolving power

1 | INTRODUCTION

Detailed characterization of highly complex mixtures at the molecular level, for example, profiling of petroleum-related samples, continues to present significant analytical challenges for high resolution mass spectrometry, which drives the development of new Fourier transform ion cyclotron resonance mass spectrometry (FT-ICR MS) instruments and data interpretation methods.[1–5] Progress in these areas has significant impact on research in the life and environmental sciences, particularly petroleomics.[6–11]

FT-ICR MS has been widely utilized in the investigation of complex natural organic matter (NOM). Mass resolving power ($m/\Delta m_{50\%}$) is one of the key analytical figures of merit for mass spectrometers; for example, petroleomics applications require a resolving power of >300 000 to distinguish mass differences of a few millidaltons (mDa): C_3 versus SH_4 (3.4 mDa) or ^{13}C versus CH (4.5 mDa). On the other hand, a resolving power of roughly 1 000 000 is required for distinguishing $^{12}C_4$ and $^{13}CSH_3$ (1.1 mDa).[12,13] In theory, the resolving power of FT-ICR MS increases linearly with the strength of the magnetic field.[14,15] However, the cost of the superconducting magnet rises quadratically with its field size. Moreover, higher field magnets usually demand more laboratory space, consume more liquid helium, and require better shimming precision. Nowadays, magnetic field strength of 9.4 Tesla or higher are required to characterize crude oil.[16–20] It would be of great benefit for the investigation of complex samples, however, if similar performances could be obtained on lower field FT-ICR instruments.

The resolving power of FT-ICR MS can be enhanced by a factor up to two by phasing the raw spectra accurately and plotting in pure absorption-mode.[21,22] This method has been successfully applied to petroleum and environmental samples.[1,23,24] Additionally, quadrupole (2ω) detection is a useful technique to improve the resolving power of FT-ICR MS at a fixed magnetic field: the first experimental implementation of arbitrary number of electrodes was described by Nikolaev and co-workers in 1985, and subsequently, Schweikhard confirmed this technique for a four electrode configuration.[25,26] In conventional FT-ICR detection mode, two cellular electrodes are used for signal detection, whereas 2ω detection utilizes four electrodes. Consequently, instruments equipped with 2ω detection offer double the resolution for a set signal acquisition time. Cho et al achieved a mass resolving power of over 1 000 000 at *m/z* 400 using a 7 T FT-ICR equipped with 2ω detection.[27] More recently, 2ω detection was successfully coupled with liquid and gas chromatography-mass spectrometry for profiling NOM.[28,29] Despite the reported higher performance, it presently remains unknown whether 2ω detection can truly replace high magnetic field FT-ICR MS instruments.

To shed some further light on the answer to this question, we evaluated 2ω detection for the analysis of a vacuum residue oil sample, by acquiring mass spectra from both 7 Tesla and 15 Tesla instruments. After determining important analytical figures of merit such as mass accuracy, resolving power, precision, signal-to-noise ratio (S/N), choice of data processing method, and so on, we found that both low and high magnetic fields have their pros and cons for the analyzed sample. To the best of our knowledge, this is the first paper systematically evaluating the performance of FT-ICR MS equipped with 2ω detection versus a conventional high field FT-ICR MS system.

2 | MATERIALS AND METHODS

2.1 | Mass spectrometry and elemental analysis

The vacuum residue oil used in this study was provided by the Research Institute of Petroleum Processing, Sinopec (Beijing, China). The sample was dissolved in toluene at 0.5 mg/mL for atmospheric pressure photoionization (APPI) in positive ion mode, as toluene assists the APPI process by absorption of photons from the krypton lamp and subsequent action as reagent ion. Full scan mass spectra were recorded using a 7T solariX 2XR FT-ICR MS (Bruker Daltonics, Bremen, Germany) equipped with 2ω detection and a 15T solariX XR FT-ICR MS (Bruker Daltonics).[30] Detailed instrumental parameters are described in Supporting Information. Briefly, spectra were both acquired from *m/z* 200 to 1500 with a transient size of 8 mega words, apodized with a Sine window function and zero-filled once. A total of 256 individual transients were collected and co-added to enhance S/N.[31] The elemental analysis of sulfur and nitrogen were performed on a Multitek sulfur analyzer (Antek, TX, USA).

2.2 | Data processing

The acquired datasets were analyzed using a combination of DataAnalysis 5.0 (Bruker Daltonics) and Composer 1.5.6 (Sierra Analytics, CA, USA) software. Identical internal calibrations were performed on the mass spectra, using CH and S_1 homologous series throughout the *m/z* range 300-1000 (calibration list is shown in Figure S1). Elemental formulae were assigned to the peaks inside the calibrated *m/z* range, with the following tolerances to filter the petroleum compounds: composition was restricted to ^{12}C(1-100), ^{1}H(1−300), ^{16}O(0−5), ^{32}S(0-2), and ^{14}N(0-3); double bond equivalents (DBE) up to 40; H/C ratio 0-2.5; O/C ratio 0-1.2; the acceptable mass error was set to ±0.5 ppm for singly charged radical ions and protonated molecules. Phase correction was performed using ftmsProcessing 2.2.0 (Bruker Daltonics) to generate the absorption-mode spectra.[32]

3 | RESULTS AND DISCUSSION

3.1 | Comparison of mass error, S/N, and elemental composition

The ICR transient and the corresponding broadband mass spectra obtained by 2ω 7T and 15T instruments are shown in Figure 1. The time-domain signal lasted up to 3.91 and 3.77 s, respectively. Interestingly, S/N of the transient from 2ω measurement was much more intense; this is because 2ω detection utilizes additional cellular electrodes in the ICR cell and records the ions' induced current four times

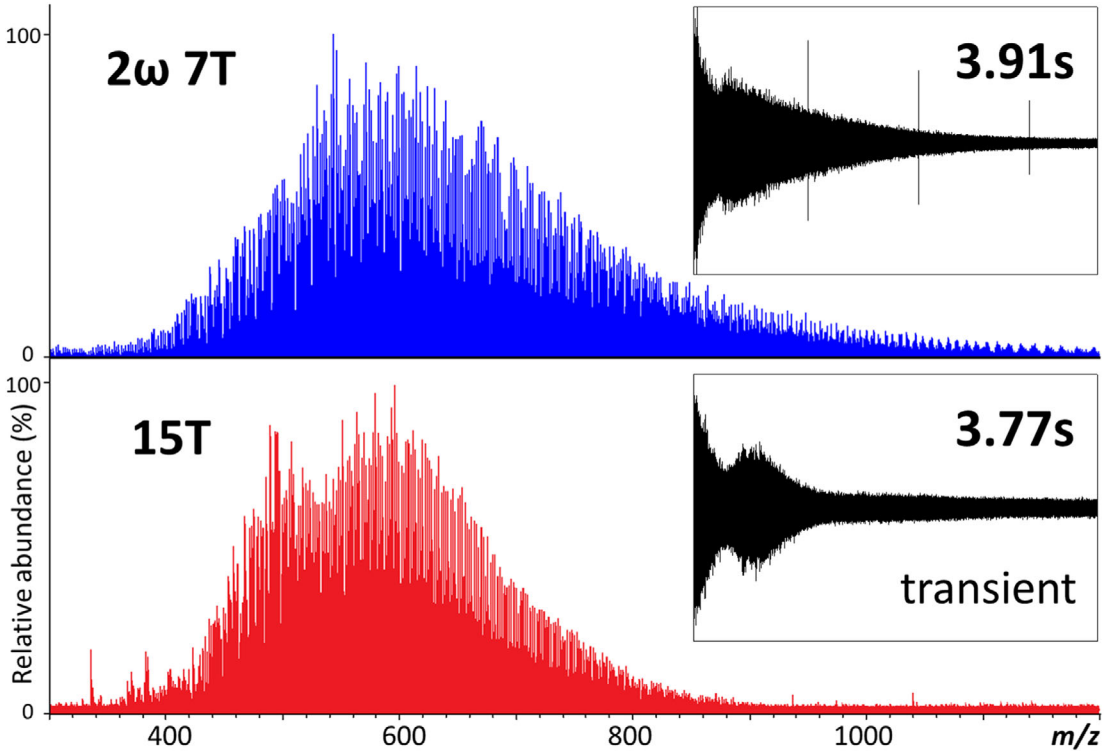

FIGURE 1 Full scan mass spectra acquired by 2ω 7T (blue) and 15T (red) FT-ICR MS for a residue oil sample, along with their ICR transients (black)

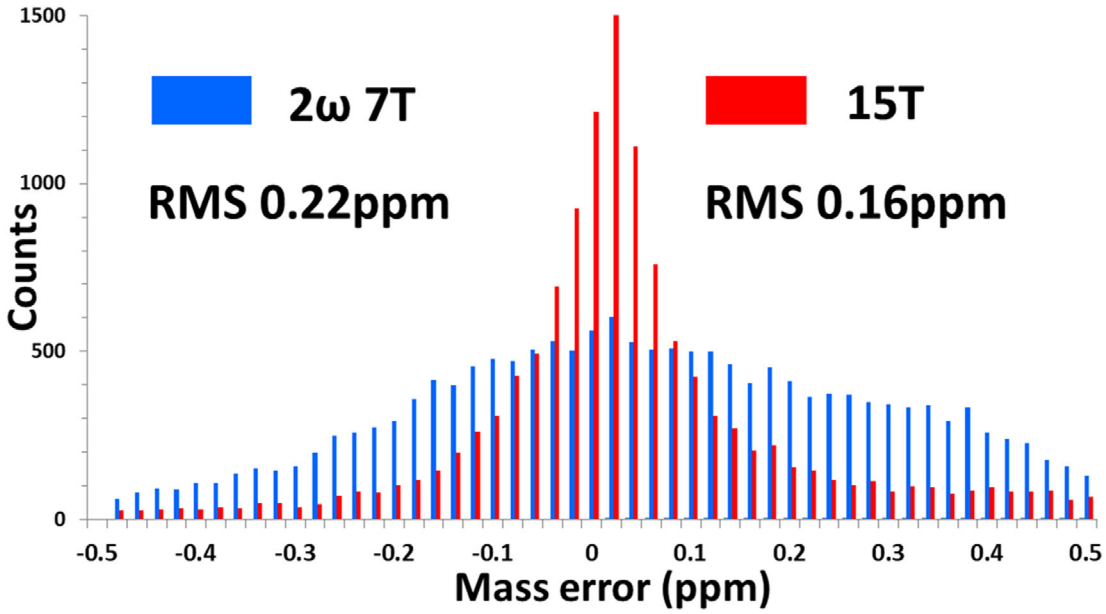

FIGURE 2 Histogram showing the mass errors of the residue oil sample measured by 2ω 7T (blue) and 15T (red) FT-ICR MS

during one ICR cycle. To better compare the results from the two mass spectra, the S/N threshold for peak picking was set to four: 16 247 peaks were assigned in the 2ω 7T spectra, whereas 12 395 were assigned in the 15T spectra. The larger proportion of assignments was resulted from the more intense transient obtained in 2ω mode, which increased S/N of the peaks, and therefore, much more low intensity species could be discerned.

Figure 2 is a histogram of the mass errors associated with the peak assignments. A normal distribution and pronounced improvement in mass accuracy were obtained by using the 15T instrument, with more

than 68% of the assignments having an associated mass error within the range of ±0.1 ppm. In contrast, only 35% of the assignments were below ±0.1 ppm in 2ω 7T detection mode. The improved mass accuracy from the 15T instrument measurements highlights the possibility of confining the window width for better formula assignments. Apart from that, a slightly positive shift of the mass errors for both instruments was observed in Figure 2, which was probably caused by space-charge effects as positive mass errors indicate that the measured ICR frequencies have a universal drift in the negative frequency direction.[33,34]

In a mass spectrum, the intensity or area of each peak represent the instrument's response to its corresponding ion current and therefore offer semi-quantitative determination of specific ion species. Based on the peak area together with its assigned elemental formulae, it is possible to estimate the relative compositions of specific elements in the sample (Table S1 lists the compositions of sulfur and nitrogen calculated from the two FT-ICR instruments and compare these compositions to traditional elemental analysis). The FT-ICR analysis here utilized APPI, which preferably ionized nonpolar, conjugated systems; it produced both protonated molecules and radical ion species. Consequently, many polyaromatic hydrocarbons and sulfur-containing components such as thiophene-based compounds in the residue oil were ionized.[13,35] In our case, such polycyclic aromatic sulfur heterocycles (PASHs) are detrimental species for the vacuum oil residue, which would not be detected unless using APPI or using electrospray ionization (ESI) following derivatization.[36,37] The estimation of S from both FT-ICR instruments was very close to the results from elemental analysis, especially from the 15T instrument. Such a phenomenon also implied that classes such as sulfide (readily protonated by ESI) are less dominated in this residue sample. This 15T advantage is due to the 15T instrument's higher resolving power to distinguish the C_4 and $^{13}CSH_3$ (1.1 mDa) species at the high *m/z* end (see next section for more details). On the other hand, the FT-ICR estimation for N was much lower as compared to elemental analysis. The nitrogen-containing compounds in the oil sample normally consist of pyrrolic (five-membered ring, acidic) and pyridinic structures (six-membered ring, basic), which are more readily ionized in ESI. Although APPI is also able to observe pyridinic and pyrrolic structures by forming protonated and radical ions simultaneously, its ionization efficiency is lower as compared to ESI. It can also induce thermal fragmentation before ion detection.[38] For this reason, the nitrogen-containing compounds are less dominant in the APPI measurements and therefore results do not truly represent the nitrogen composition of a sample.

3.2 | Mass resolving power and performance for individual compound classes

In theory, the mass resolving power of FT-ICR increases linearly with the applied magnetic field strength. As the quadrupole detection mode can double the resolving power for a given magnetic field, the two instruments investigated here should offer comparable performance. In our experiments, the resolving powers were calculated from both 7 and 15T mass spectra, showing that the mass resolving powers decreased by a factor approximately equal to *m/z*, and a resolving power of almost 1 000 000 was seen at *m/z* 400 for spectra from both instruments (an example is shown in Figure S2). In petroleum samples, compounds appear in regular patterns according to their hydrogen deficiency, heteroatom content, and carbon distribution. In our analyses, a resolving power of >400 000 was still be achieved at *m/z* 900, demonstrating that the 2ω 7T instrument has the ability to distinguish the small mass difference between C_3 and SH_4 (3.4 mDa) even at the high *m/z* end (Figure 3), which is an important prerequisite for petroleum studies. Apart from this important mass difference, which is widely used as a benchmark for the capabilities of a FT-ICR system,[1,24] another characteristic mass difference was also seen for the difference of C_4 and $^{13}CSH_4$, corresponding to 1.1 mDa. This Δmass is seen in APPI spectra where both even and odd electron ions are produced. In Figure 3, *m/z* windows of ~10 mDa were expanded for representative compounds to compare the performance of the two FT-ICR instruments. At *m/z* of 448.2186, the elemental formula of $[C_{35}H_{28}]^{\cdot+}$ was calculated, with a small adjacent isobaric signal at *m/z* 448.2175 ($[C_{31}{}^{13}CH_{30}S+H]^+$) with 1.1 mDa distance (C_4 and $^{13}CSH_4$). The two peaks were successfully resolved from both mass spectra. Generally, differences of the two instruments were less pronounced in the lower *m/z* end. At higher *m/z* values, however, this issue became significant due to the sharp decrease of mass resolving power and the large increase of possible elemental compositions. As illustrated in Figure 3 (right) for *m/z* 812.7194, the wide sideband extending from the large $[C_{60}H_{92}]^{\cdot+}$ peak interfered and overlapped with the low abundant $[C_{56}{}^{13}CH_{94}S+H]^+$ ion species nearby for the 2ω 7T instrument. This phenomenon is called "peak coalescence," which occurs when two ion clouds have very similar *m/z*. This issue can be overcome by increasing the magnetic field.[14] By utilizing the 15T instrument, the C_4 and $^{13}CSH_4$ ion species at the high *m/z* end were almost baseline resolved, along with greatly improved mass accuracy. However, it should also be pointed out that the minute mass difference of 1.1 mDa is generally of minor importance, as the $^{13}CSH_4$ species is an additional isotopic signal; hence, the number of compound assignments does not increase by using the additional $^{13}CSH_4$ peak assignments.

To further explore the two instruments' performances for individual compound classes, DBE versus carbon number plots of the S_1 radical ion class ($[C_xH_yS_1]^{\cdot+}$) were generated (Figure 4). It was immediately obvious that the chemical compositions distributed continuously in both plots (2ω 7T versus 15T) and almost no gap was observed. The upper plot for the 2ω 7T showed a wider distribution because the 2ω mode was able to record more intense ion signals, resulting in a larger number of compounds detected. Although the 15T instrument was able to resolve the 1.1 mDa mass difference of C_4 and $^{13}CSH_3$ throughout the entire *m/z* range, the additional isotope signal of the $^{13}CSH_3$ species did not offer extra compound assignments (vide supra). A detailed view of the DBE distribution revealed more intense contributions from 6, 9, and 12 DBE, indicating favored individual compound structures of the $[C_xH_yS_1]^{\cdot+}$ radical species during APPI ionization, and thus providing additional structural insight. In petroleomics

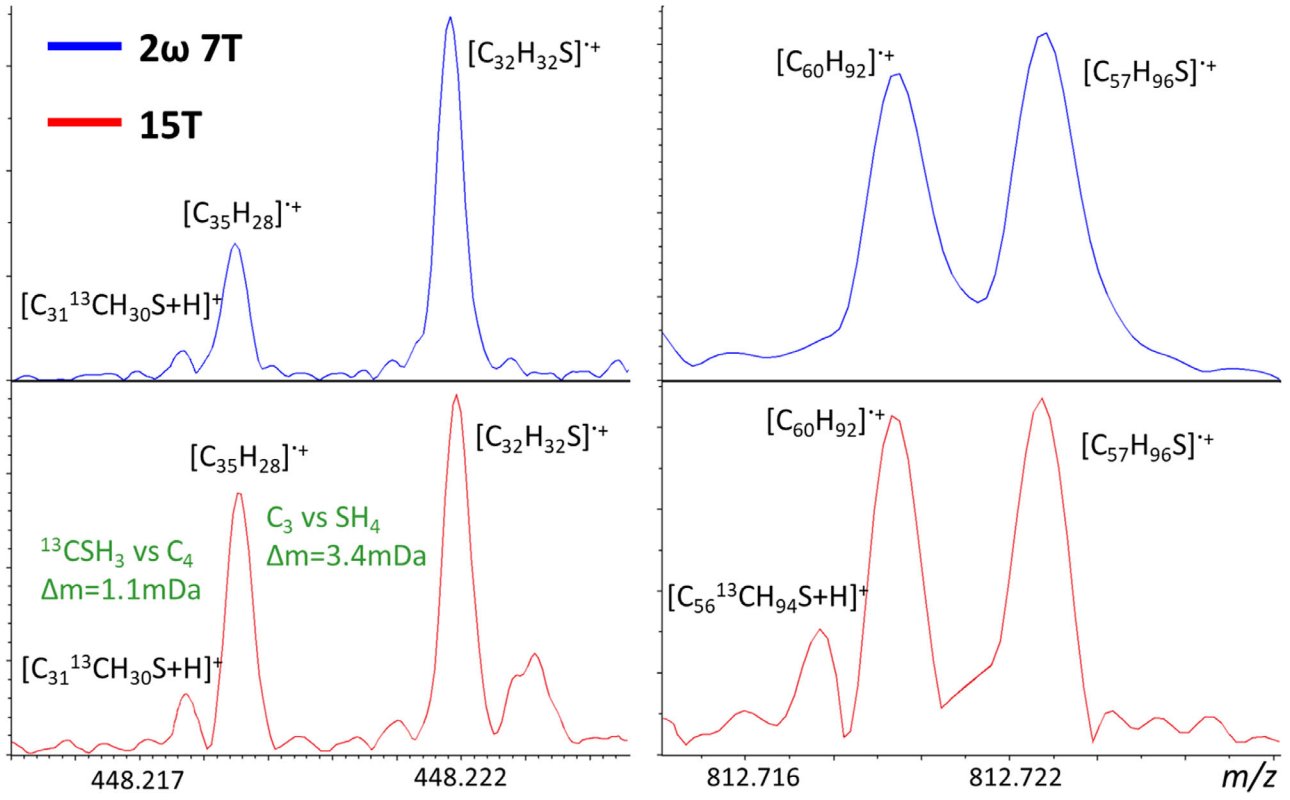

FIGURE 3 Mass scale expansions of two adjacent peaks (C_3 versus SH_4, 3.4 mDa) and (C_4 versus $^{13}CSH_3$, 1.1 mDa) from mass spectra acquired by 2ω 7T (blue) and 15T (red) FT-ICR MS

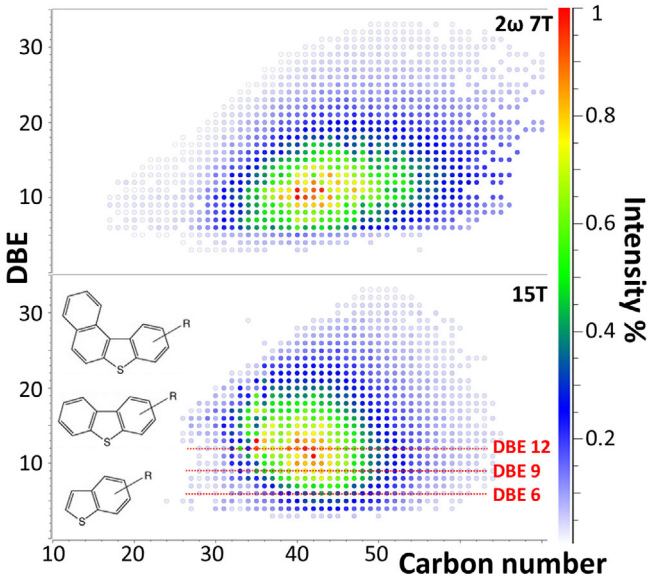

FIGURE 4 DBE versus carbon number distribution plots for the S_1 compound class radical ions observed from 2ω 7T (top) and 15T (bottom) FT-ICR MS, with possible alkylated thiophenic structures proposed for the compounds with DBE of 6, 9, and 12

studies, this distribution corresponds to the well-known thiophenic core.[39] For the S_1 radical ion class investigated here, a DBE of 6, 9, and 12 correlates with alkylated benzothiophenes, dibenzothiophenes, and benzonaphthothiophene, respectively (Figure 4), demonstrating that these three aromatic cores are likely present in the vacuum oil residue. In addition, Figure 4 also shows the lack of S_1 species of DBE values between 0 and 5; indicating that compounds such as sulfides, thiophenes, naphthenothiophenes, and cycloalkenothiophenes are less abundant in the sample.[40–42]

Importantly, it was shown that both instruments have the ability to comprehensively characterize the thiophene-based compounds and polycyclic aromatic hydrocarbons in a complex mixture. A wide carbon number range was recorded by the 2ω 7T instrument due to the higher signal intensities.

3.3 | Phase correction

Magnitude and absorption-mode processing are two different modes to display FT-ICR mass spectra. Most often, magnitude-mode is used, where absolute values of the complex output after the Fourier transform are plotted. In absorption-mode, the real part of the complex output is plotted by considering the accurate phase value of each ion signal. It has been recognized that absorption-mode spectra offer up to a two-fold increase in mass resolving power and $\sqrt{2}$-fold increase in the S/N compared to the conventional magnitude-mode.[31,43–45] In this study, the mass spectra acquired from the two instruments were processed using a commercial software (ftmsProcessing 2.2.0) for absorption-mode spectra generation. Unfortunately, a negative baseline drift was observed in the absorption-mode spectra recorded

from the 15T instrument, which would severely distort spectral quality and subsequent data interpretation (an example is shown in Figure S3). In contrast, the absorption-mode spectrum from the 2ω 7T instrument showed a much flatter and smoother baseline and lead to an approximately two-fold improvement in the spectral quality. As the peak shapes resulting from the Fourier transform are a convolution of a "Sinc" and a "Lorentzian" functions, the slight wiggles seen in the spectra are actually characteristic of an absorption-mode spectrum.[46] For absorption-mode processing, a function in which the ions' phases accumulated quadratically with their cyclotron frequencies is required to precisely correct the phase shifts for each data point in the spectrum.[31] For example, an ion with *m/z* of 250 corresponds to a frequency of 860 000 Hz in a 7T instrument; this value will be 920 000 Hz in a 15T instrument. Consequently, after quadratical accumulation, a much more complex phase shift is expected in a 15T instrument, leading to the unusual negative wiggles in the baseline. Normally, additional data processing such as windowing function, baseline correction and peak-picking algorithms would be required to overcome such an issue.[21,47–50] For this reason, the additional efforts of spectrum handling for the absorption-mode may not always be worthwhile for performing phase correction on a high magnetic field FT-ICR instrument.

4 | CONCLUSIONS

Quadrupole detection is an important complementary technique for FT-ICR MS for the study of complex mixtures at the molecular level, especially for instruments with small magnetic fields. This work demonstrates that 2ω 7T FT-ICR MS offered comparable mass resolving power and even higher compound assignment rates as compared to the 15T FT-ICR MS and therefore produced more continuous DBE and carbon number distributions. On the other hand, the measurements from 15T FT-ICR MS were more precise and therefore gave improved reliability of peak assignments and better estimation of elemental compositions for the investigated sample. In addition, phase correction was also examined for the two instruments, but additional efforts are required for the 15T FT-ICR MS to generate spectra in the absorption-mode. In summary, we believe that this work represents an important contribution to scientists and users interested in the comparison of the performance of different FT-ICR instruments.

ACKNOWLEDGMENTS

Y.Q and S.L. are both grateful for the funding by the National Natural Science Foundation of China (42007290 and 41925002). D.A.V. acknowledges research support by the German Research Foundation (DFG VO 1355/4-3). The authors are grateful for the valuable comments from the anonymous reviewers.

AUTHOR CONTRIBUTIONS

The manuscript was written through contributions of all authors.

CONFLICTS OF INTEREST

The authors declare no competing financial and nonfinancial interests. D.A.V. is Editor-in-Chief of Analytical Science Advances.

REFERENCES

1. Cho Y, Qi Y, O'Connor PB, Barrow MP, Kim S. Application of phase correction to improve the interpretation of crude oil spectra obtained using 7 T Fourier transform ion cyclotron resonance mass spectrometry. *J Am Soc Mass Spectrom*. 2014;25(1):154-157.
2. Headley JV, Peru KM, Barrow MP. Advances in mass spectrometric characterization of naphthenic acids fraction compounds in oil sands environmental samples and crude oil-a review. *Mass Spectrom Rev*. 2015;35(2):311-328.
3. Qi Y, Hempelmann R, Volmer DA. Two-dimensional mass defect matrix plots for mapping genealogical links in mixtures of lignin depolymerisation products. *Anal Bioanal Chem*. 2016;408(18):4835-4843.
4. Hughey CA, Hendrickson CL, Rodgers RP, Marshall AG, Qian K. Kendrick mass defect spectrum: a compact visual analysis for ultrahigh-resolution broadband mass spectra. *Anal Chem*. 2001;73(19):4676-4681.
5. Kim S, Kramer RW, Hatcher PG. Graphical method for analysis of ultrahigh-resolution broadband mass spectra of natural organic matter, the Van Krevelen diagram. *Anal Chem*. 2003;75(20):5336-5344.
6. Wagner S, Riedel T, Niggemann J, Vähätalo AV, Dittmar T, Jaffé R. Linking the molecular signature of heteroatomic dissolved organic matter to watershed characteristics in world rivers. *Environ Sci Technol*. 2015;49(23):13798-13806.
7. Palacio Lozano CD, Thomas MJ, Jones HE, Barrow MP. Petroleomics: tools, challenges, and developments. *Annu Rev Anal Chem*. 2020;13(1):405-430.
8. Qi Y, Fu P, Volmer DA. analysis of natural organic matter via fourier transform ion cyclotron resonance mass spectrometry: an overview of recent non-petroleum applications. *Mass Spectrom Rev*. 2020.
9. Qi Y, Volmer DA. Electron-based fragmentation methods in mass spectrometry: an overview. *Mass Spectrom Rev*. 2017;36(1):4-15.
10. Qi Y, Volmer DA. Rapid mass spectral fingerprinting of complex mixtures of decomposed lignin: data-processing methods for high-resolution full-scan mass spectra. *Rapid Commun Mass Spectrom*. 2018;33:2-10.
11. Headley JV, Peru KM, Barrow MP. Mass spectrometric characterization of naphthenic acids in environmental samples: a review. *Mass Spectrom Rev*. 2009;28(1):121-134.
12. Hsu CS, Hendrickson CL, Rodgers RP, McKenna AM, Marshall AG. Petroleomics: advanced molecular probe for petroleum heavy ends. *J Mass Spectrom*. 2011;46(4):337-343.
13. Purcell JM, Hendrickson CL, Rodgers RP, Marshall AG. Atmospheric pressure photoionization fourier transform ion cyclotron resonance mass spectrometry for complex mixture analysis. *Anal Chem*. 2006;78(16):5906-5912.
14. Marshall AG, Hendrickson CL, Jackson GS. Fourier transform ion cyclotron resonance mass spectrometry: a primer. *Mass Spectrom Rev*. 1998;17(1):1-35.
15. Jonathan Amster I. Fourier transform mass spectrometry. *J Mass Spectrom*. 1996;31(12):1325-1337.
16. Barrow MP, Witt M, Headley JV, Peru KM. Athabasca oil sands process water: characterization by atmospheric pressure photoionization and electrospray ionization Fourier transform ion cyclotron resonance mass spectrometry. *Anal Chem*. 2010;82(9):3727-3735.
17. McKenna AM, Purcell JM, Rodgers RP, Marshall AG. Heavy petroleum composition. 1. Exhaustive compositional analysis of athabasca bitumen HVGO distillates by fourier transform ion cyclotron resonance mass spectrometry: a definitive test of the Boduszynski model. *Energy Fuels*. 2010;24(5):2929-2938.

18. Gaspar A, Zellermann E, Lababidi S, Reece J, Schrader W. Impact of different ionization methods on the molecular assignments of asphaltenes by FT-ICR mass spectrometry. *Anal Chem*. 2012;84(12):5257-5267.
19. Bae E, Na J-G, Chung SH, Kim HS, Kim S. Identification of about 30 000 chemical components in shale oils by electrospray ionization (ESI) and atmospheric pressure photoionization (APPI) coupled with 15 T Fourier transform ion cyclotron resonance mass spectrometry (FT-ICR MS) and a comparison to conventional oils. *Energy Fuels*. 2010;24(4):2563-2569.
20. Shi Q, Zhao S, Xu Z, Chung KH, Zhang Y, Xu C. Distribution of acids and neutral nitrogen compounds in a chinese crude oil and its fractions: characterized by negative-ion electrospray ionization Fourier transform ion cyclotron resonance mass spectrometry. *Energy Fuels*. 2010;24(7):4005-4011.
21. Xian F, Hendrickson CL, Blakney GT, Beu SC, Marshall AG. Automated broadband phase correction of Fourier transform ion cyclotron resonance mass spectra. *Anal Chem*. 2010;82(21):8807-8812.
22. Qi Y, Barrow MP, Van Orden SL, et al. Variation of the Fourier transform mass spectra phase function with experimental parameters. *Anal Chem*. 2011;83(22):8477-8483.
23. Silva Da, P M, Kaesler JM, Reemtsma T, Lechtenfeld OJ. Absorption mode spectral processing improves data quality of natural organic matter analysis by Fourier-transform ion cyclotron resonance mass spectrometry. *J Am Soc Mass Spectrom*. 2020;31(7):1615-1618.
24. Qi Y, Luo R, Schrader W, Volmer DA. Application of phase correction to improve the characterization of photooxidation products of lignin using 7 Tesla Fourier-transform ion cyclotron resonance mass spectrometry. *FACETS*. 2017;2(2):461-475.
25. Nikolaev EN, Gorshkov MV, Mordehai AV, Talrose VL. Ion cyclotron resonance signal-detection at multiples of the cyclotron frequency. *Rapid Commun Mass Spectrom*. 1990;4(5):144-146.
26. Schweikhard L. Theory of quadrupole detection Fourier transform-ion cyclotron resonance. *Int J Mass Spectrom Ion Process*. 1991;107(2):281-292.
27. Cho E, Witt M, Hur M, Jung M-J, Kim S. Application of FT-ICR MS equipped with quadrupole detection for analysis of crude oil. *Anal Chem*. 2017;89(22):12101-12107.
28. Kim D, Kim S, Son S, Jung M-J, Kim S. Application of online liquid chromatography 7 T FT-ICR mass spectrometer equipped with quadrupolar detection for analysis of natural organic matter. *Anal Chem*. 2019;91(12):7690-7697.
29. Thomas MJ, Collinge E, Witt M, et al. Petroleomic depth profiling of Staten Island salt marsh soil: 2ω detection FTICR MS offers a new solution for the analysis of environmental contaminants. *Sci Total Environ*. 2019;662:852-862.
30. Nikolaev EN, Boldin IA, Jertz R, Baykut G. Initial experimental characterization of a new ultra-high resolution FTICR cell with dynamic harmonization. *J Am Soc Mass Spectrom*. 2011;22(7):1125-1133.
31. Qi Y, O'Connor PB. Data processing in Fourier transform ion cyclotron resonance mass spectrometry. *Mass Spectrom Rev*. 2014;33(5):333-352.
32. Qi Y, Thompson CJ, Van Orden SL, O'Connor PB. Phase correction of Fourier transform ion cyclotron resonance mass spectra using MatLab. *J Am Soc Mass Spectrom*. 2011;22(1):138-147.
33. Ledford EB, Ghaderi S, White RL, et al. Exact mass measurement by Fourier transform mass spectrometry. *Anal Chem*. 1980;52(3):463-468.
34. Aizikov K, Mathur R, O'Connor PB. The spontaneous loss of coherence catastrophe in Fourier transform ion cyclotron resonance mass spectrometry. *J Am Soc Mass Spectrom*. 2009;20(2):247-256.
35. Qi Y, Fu P, Li S, Ma C, Liu C, Volmer DA. Assessment of molecular diversity of lignin products by various ionization techniques and high-resolution mass spectrometry. *Sci Total Environ*. 2020;713:136573.
36. Hourani N, Andersson JT, Möller I, Amad M, Witt M, Sarathy SM. Atmospheric pressure chemical ionization Fourier transform ion cyclotron resonance mass spectrometry for complex thiophenic mixture analysis. *Rapid Commun Mass Spectrom*. 2013';27(21):2432-2438.
37. Panda SK, Andersson JT, Schrader W. Characterization of supercomplex crude oil mixtures: what is really in there? *Angew Chemie Int Ed*. 2009;48(10):1788-1791.
38. Purcell JM, Rodgers RP, Hendrickson CL, Marshall AG. Speciation of nitrogen containing aromatics by atmospheric pressure photoionization or electrospray ionization Fourier transform ion cyclotron resonance mass spectrometry. *J Am Soc Mass Spectrom*. 2007;18(7):1265-1273.
39. Griffiths MT, Da Campo R, O'Connor PB, Barrow MP. Throwing light on petroleum: simulated exposure of crude oil to sunlight and characterization using atmospheric pressure photoionization Fourier transform ion cyclotron resonance mass spectrometry. *Anal Chem*. 2014;86(1):527-534.
40. Liu P, Xu C, Shi Q, et al. Characterization of sulfide compounds in petroleum: selective oxidation followed by positive-ion electrospray Fourier transform ion cyclotron resonance mass spectrometry. *Anal Chem*. 2010;82(15):6601-6606.
41. Vetere A, Pröfrock D, Schrader W. Quantitative and qualitative analysis of three classes of sulfur compounds in crude oil. *Angew Chemie Int Ed*. 2017;56(36):10933-10937.
42. Qi Y, Volmer DA. Chemical diversity of lignin degradation products revealed by matrix-optimized MALDI mass spectrometry. *Anal Bioanal Chem*. 2019;411(23):6031-6037.
43. Qi Y, Barrow MP, Li H, et al. Absorption-mode: the next generation of Fourier transform mass spectra. *Anal Chem*. 2012;84(6):2923-2929.
44. Qi Y, Witt M, Jertz R, et al. Absorption-mode spectra on the dynamically harmonized Fourier transform ion cyclotron resonance cell. *Rapid Commun Mass Spectrom*. 2012;26(17):2021-2026.
45. Kilgour DPA, Wills R, Qi Y, O'Connor PB. Autophaser: an algorithm for automated generation of absorption mode spectra for FT-ICR MS. *Anal Chem*. 2013;85(8):3903-3911.
46. Marshall AG, Comisarow MB, Parisod G. Relaxation and spectral line shape in Fourier transform ion resonance spectroscopy. *J Chem Phys*. 1979;71(11):4434-4444.
47. Kilgour DPA, Van Orden SL. Absorption mode Fourier transform mass spectrometry with no baseline correction using a novel asymmetric apodization function. *Rapid Commun Mass Spectrom*. 2015;29(11):1009-1018.
48. Qi Y, Li H, Wills RH, et al. Absorption-mode Fourier transform mass spectrometry: the effects of apodization and phasing on modified protein spectra. *J Am Soc Mass Spectrom*. 2013;24(6):828-834.
49. Xian F, Corilo YE, Hendrickson CL, Marshall AG. Baseline correction of absorption-mode Fourier transform ion cyclotron resonance mass spectra. *Int J Mass Spectrom*. 2012;325-327:67-72.
50. Lee JP, Comisarow MB. Advantageous apodization functions for absorption-mode Fourier transform spectroscopy. *Appl Spectrosc*. 1989;43(4):599-604.

SUPPORTING INFORMATION

Additional supporting information may be found online in the Supporting Information section at the end of the article.

How to cite this article: Ge J, Ma C, Qi Y, et al. Quadrupole detection FT-ICR mass spectrometry offers deep profiling of residue oil: a systematic comparison of 2ω 7 Tesla versus 15 Tesla instruments. *Anal Sci Adv*. 2021;2:272–278. https://doi.org/10.1002/ansa.202000123